Continuous Copolymerization of Vinylidene Fluoride with Hexafluoropropylene in Supercritical Carbon Dioxide: High-Hexafluoropropylene-Content Amorphous Copolymers

Tamer S. Ahmed,[†] Joseph M. DeSimone,[†,‡] and George W. Roberts*[,†]

Department of Chemical and Biomolecular Engineering, North Carolina State University, Box 7905, Raleigh, North Carolina 27695-7905, and Department of Chemistry, University of North Carolina at Chapel Hill, Box 3290, Chapel Hill, North Carolina 27599-3290

Received November 13, 2007; In Final Form February 13, 2008; Revised Manuscript Received February 11, 2008

ABSTRACT: Copolymerization of vinylidene fluoride (VF2) and hexafluoropropylene (HFP) was carried out in supercritical carbon dioxide using a continuous stirred tank reactor. Three different HFP/VF2 molar feed ratios were studied, 59:41, 66:34, and 73:27, giving rise to amorphous copolymers containing about 23, 26, and 30 mol % HFP, respectively. The experiments were carried out at 40 °C with pressures in the range of 207–400 bar using perfluorobutyryl peroxide as the free radical initiator. Depending on the copolymer composition, the molecular weight, and the reaction pressure, either a homogeneous (solution) or a heterogeneous (precipitation) polymerization was observed. The effects of feed monomer concentration and reaction pressure were explored at otherwise constant conditions. The rate of polymerization (R_p) and the number-average molecular weight (M_n) increased linearly with the total monomer concentration, independent of the mode of polymerization, i.e., homogeneous or heterogeneous. Both R_p and M_n increased by about 20–30% when the reaction pressure was increased from 207 to 400 bar. This increase could be accounted for by the effect of pressure on the reaction rate constants. The molecular weight distributions were perfectly unimodal except for the lowest HFP-content copolymers at the highest monomer concentrations. The data suggest that the carbon-dioxide-rich fluid phase is the main locus of polymerization, even when the polymer precipitates during the reaction.

Introduction

Since their discovery in 1957 by DuPont de Nemours Company,[1] copolymers of vinylidene fluoride (VF2) with hexafluoropropylene (HFP) have found use in many applications. When the HFP content of the copolymer is in the range of 5–15 mol%, the copolymers show thermoplastic properties and are called "flexible PVDF". For HFP contents higher than about 20 mol%, the copolymers are amorphous and elastomeric.[2,3] The maximum theoretical incorporation of HFP in the copolymer is restricted to 50 mol% since HFP has a zero reactivity ratio.[4–6]

Thermoplastic VF2−HFP copolymers are produced commercially by either emulsion or suspension polymerizations in water,[7,8] while the elastomeric VF2−HFP copolymers are produced only by aqueous emulsion polymerization[1,2,9,10] because of their tacky nature.[11] Both processes generate large quantities of wastewater and require large quantities of energy to isolate the polymer in a dry form. Moreover, the emulsion technique involves the use of perfluorooctanoic acid (PFOA)-based surfactants especially for high solid-content loadings.[12] These fluorinated surfactants are of environmental concern since they are nonbiodegradable and bioaccumulate in human fatty tissues.[13] In addition, their future availability is uncertain.[14] Polymerization in supercritical carbon dioxide ($scCO_2$) is the only known alternative that can eliminate the need for PFOA-based surfactants in the manufacturing process.[15]

In a recent publication,[16] we described the use of continuous precipitation polymerization to synthesize low-HFP-content poly(VF2-*co*-HFP) containing about 9.2 mol % HFP. The Introduction section of that publication described in detail the properties of $scCO_2$, the incentives for using it as a polymerization medium, the rationale for continuous operation, and the uses and manufacturing processes for commercial poly(VF2-*co*-HFP) products.

The current publication describes the synthesis of amorphous copolymers of VF2 and HFP containing from 23 to 30 mol % HFP via continuous polymerization in $scCO_2$. The behavior of these polymerizations differs from those of the low-HFP-content copolymers[16] and from VF2 homopolymers (PVDF).[17–20] In particular, some of the polymerizations are heterogeneous, i.e., polymer precipitates during the reaction, whereas some are homogeneous. These differences required modification of the experimental equipment. Nevertheless, the differences helped to illuminate the polymerization mechanism over a broader range of conditions. Moreover, the data for the high-HFP-content polymerizations shed additional light on the important issue of where the polymerization actually takes place.[16]

Experimental Section

Materials. Carbon dioxide (SFC grade, 99.998%, max O_2 = 2 ppm) and argon (99.9999%) were obtained from National Specialty Gases. To completely remove O_2 from the CO_2, three Alltech High Pressure Oxy-Trap traps were installed in parallel between the CO_2 tanks and the CO_2 pump. Both VF2 (99% min, balance N_2) and HFP (99% min, balance N_2) were obtained from SynQuest Laboratories. An Alltech High Pressure Oxy-Trap trap was installed between each monomer cylinder and its corresponding pump. All other chemicals were obtained from Fisher Scientific and used as received.

Initiator Synthesis. Perfluorobutyryl peroxide ($[C_3F_7COO]_2$, PBP) was synthesized in 1,1,2-trichloro-1,2,2-trifluoroethane (HPLC-grade, 99.8%, Freon 113) as previously reported.[21] All manipulations of the initiator were performed in a NaCl/ice bath, and the final product was stored under dry ice. The iodine titration technique, ASTM Method E 298-91, was utilized to determine the concentration of the initiator in the solution. The initiator concentra-

* To whom correspondence should be addressed. Tel: +1-919-515-7328. Fax: +1-919-515-3465. E-mail: groberts@eos.ncsu.edu.
† North Carolina State University.
‡ University of North Carolina at Chapel Hill.

10.1021/ma702526u CCC: $40.75
Published on Web 04/15/2008

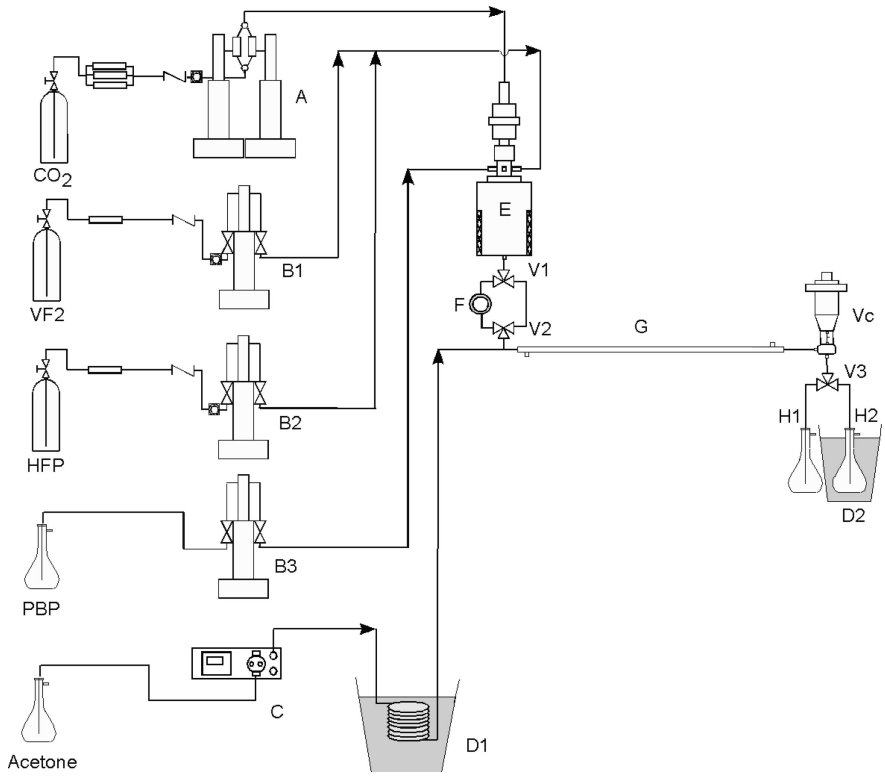

Figure 1. CSTR polymerization system: A, continuous syringe pump; B1,B2,B3, syringe pumps; C, HPLC pump; D1,D2, dry ice/acetone baths; E, autoclave with stirrer; F, view cell; G, heat exchanger; H1,H2, glass flasks; V1,V2,V3, three-way valves; Vc, control valve.

tion was reduced to 0.03 M by dilution with additional Freon 113 before use. After a second titration, the initiator solution was introduced to the initiator pump under an argon blanket. The half-life of PBP in Freon 113 is about 35 min at 40 °C.[21]

Polymerization Apparatus and Procedure. Figure 1 shows a schematic of the continuous polymerization system. The reactor (E) is a 100 mL high-pressure autoclave (Autoclave Engineers) with a magnetically driven agitator (Autoclave Engineers). Three downward-pumping impellers were mounted on the shaft of the agitator. The current autoclave has the same length-to-diameter ratio as the 800 mL reactor used for PVDF[17–20] and poly(acrylic acid)[22–24] and is the same one used for low-HFP-content poly(VF2-*co*-HFP).[16] An HPLC pump (C, Alltech 301 HPLC pump) was used to inject acetone continuously into the effluent from the reactor (E). The acetone was cooled in a dry ice/acetone bath before it was injected. McHugh et al.[25] reported that acetone acted as a cosolvent with CO_2 to reduce the cloud-point curve of poly(VF2-*co*-HFP) containing about 22 mol% HFP to near atmospheric pressure for temperatures below 10 °C. The purpose of cold acetone injection in these experiments was to increase the solubility of the copolymer in the effluent mixture to facilitate passing the effluent stream through the control valve (Vc). Thus, a continuous stream of acetone with the copolymer dissolved in it was collected into one of two flasks (H1, H2). The precooling of the acetone stream helped to prevent chain transfer to acetone and to minimize post polymerization. This was especially important since PBP is a very active initiator.[21] In addition, a heat exchanger (G) with a cold refrigerant (−10 °C) was used to reduce initiator decomposition and post polymerization.

In a typical experiment, the reactor (E) and the lines were purged three times with CO_2 at about 103 bar to remove oxygen. Syringe pumps A, B1 (cooled by 15 °C refrigerant), B2 (cooled by 15 °C refrigerant), B3 (cooled by –7.5 °C refrigerant), and C were used to feed CO_2, VF2, HFP, PBP solution, and acetone, respectively. The effect of pressure on the monomer densities that were used to calculate the flow rates out of the pumps was taken into account using the Hakinson−Brobst−Thomson method.[26,27] The speed of the reactor agitator was fixed at 2000 rpm in all the runs. Two three-way ball valves (V1 and V2) were used to direct the effluent from the reactor either to a high-pressure view cell (F) or to normal tubing. The view cell was used to monitor the phase of the effluent from the reactor to determine if the polymer had precipitated in the reactor. The view cell was also used to determine the cloud-point pressure of the reaction mixture. The temperature of the view cell and all tubing connecting it to the reactor was maintained at reactor temperature. The effluent stream containing the injected acetone was directed by another three-way valve (V3) to either the unsteady-state (H1) or the steady-state (H2) collection flasks. The unreacted monomers and CO_2 were purged through an opening in each flask while acetone/copolymer solution was collected. The acetone/copolymer solution was collected for at least one average residence time after steady state was attained. In addition, the steady-state flask (H2) was maintained in a dry ice/acetone bath to prevent post polymerization. After the steady-state collection, valve V3 was switched back to the unsteady-state flask (H1) and the view cell (F) was connected to the system using valves V1 and V2 to monitor the phase of the reaction mixture. If the reaction mixture was homogeneous, the pressure was decreased slowly to determine the cloud-point pressure (CPP), defined as the pressure at which the solution becomes so opaque that the magnetic stirrer in the view cell can no longer be seen. Cloud points obtained in this manner are generally very close to those defined as the point where there is a 90% drop in transmitted light through the solution.[28] The system was then shut down, and the residual monomers were purged from the acetone solution by bubbling argon into the solution for at least 30 min. Acetone was then evaporated and the collected copolymer was kept at 50 °C in a vacuum oven for at least 12 h to remove acetone and/or monomers residuals.

Characterization. Gel permeation chromatography (GPC) was performed at 40 °C using a Waters 150-CV GPC equipped with Waters Styragel HR 5, 4, 2, and 0.5 columns and a refractive index detector. Tetrahydrofuran was used as the mobile phase, and polystyrene standards were used for the calibration.

Hydrogen, carbon, and fluorine elemental analyses were performed by Atlantic Microlab, Inc. Hydrogen and carbon analyses were performed by combustion using automatic analyzers, while

Table 1. Effect of Inlet Total Monomer Concentration on the Continuous Copolymerization of High-HFP-Content VF2/HFP Copolymers in $scCO_2$[a]

no.	HFP/VF2 molar feed ratio	$[M_T]_{in}$ (mol/L)	$[F_{HFP}]_{F\text{-}EA}$ (mol %)[b]	$[F_{HFP}]_{NMR}$ (mol %)[c]	$(R_P)_{av}$ (10^{-2} mol/L·min)[d]	$[M_T]_{out\text{-}av}$ (mol/L)[e]	$(M_n)_{NMR}$(kDa)[f]	$(M_n)_{GPC}$ (kDa)	PDI	reaction medium and CPP[g]
1	59:41	1.5	23.7 ± 1.35	22.4	0.72	1.36	14.4	14.7	1.5	homogenous (CPP = 303 bar)
2	59:41	3.6	24.2 ± 1.36	22.6	1.58	3.28	32.2	29.5	1.5	heterogeneous
3	59:41	5.2	23.7 ± 1.35	22.8	2.16	4.80	48.8	45.6	1.5	heterogeneous
4	59:41	6.5	24.4 ± 1.36	22.8	3.07	5.89	67.4	59.8	1.6	heterogeneous
5	66:34	1.5	27.0 ± 1.43	25.9	0.64	1.37	13.3	13.7	1.5	homogenous (CPP = 271 bar)
6	66:34	3.6	26.4 ± 1.42	26.1	1.43	3.31	30.6	29.2	1.5	homogenous (CPP = 352 bar)
7	66:34	5.2	26.4 ± 1.44	26.3	2.20	4.79	44.7	44.3	1.5	heterogeneous
8	66:34	6.5	26.2 ± 1.44	26.4	2.59	5.98	60.9	52.7	1.5	heterogeneous
9	73:27	1.5	30.3 ± 1.53	28.9	0.55	1.39	12.0	12.3	1.5	homogenous (CPP = 231 bar)
10	73:27	3.6	31.8 ± 1.58	29.2	1.41	3.32	31.9	29.0	1.5	homogenous (CPP = 291 bar)
11	73:27	5.2	31.8 ± 1.57	29.3	2.20	4.79	49.9	46.5	1.5	homogenous (CPP = 331 bar)
12	73:27	6.5	30.8 ± 1.57	30.1	2.71	5.96	63.2	57.1	1.5	homogenous (CPP = 372 bar)

[a] Reaction conditions: $P = 400$ bar; $T = 40$ °C; $\tau = 20$ min; $[I]_{in} = 0.003$ M. For the three feed ratios, the average inlet $scCO_2$ concentration ranges from 87.8 mol % at 1.5 mol/L $[M_T]_{in}$ to 50.5 mol % at 6.5 mol/L $[M_T]_{in}$. [b] HFP incorporation in the copolymer from fluorine elemental analysis (eq 3); The error limit in $[F_{HFP}]_{F\text{-}EA}$ corresponds to the ±0.3 wt % accuracy and precision error. [c] HFP incorporation in the copolymer from NMR (eq 4). [d] Average molar rate of polymerization based on the average of $[F_{HFP}]_{F\text{-}EA}$ and $[F_{HFP}]_{NMR}$ (eq 1). [e] Average total monomer concentration inside the reactor and in the effluent based on the average of $[F_{HFP}]_{F\text{-}EA}$ and $[F_{HFP}]_{NMR}$ (eq 2). [f] Number-average molecular weight calculated from initiator end-group analysis by NMR (eq 5). [g] CPP = Cloud-point pressure.

Table 2. Effect of Reaction Pressure on the Continuous Copolymerization of High-HFP-Content VF2/HFP Copolymers in $scCO_2$[a]

no.	HFP/VF2 mol-feed-ratio	P (bar)	$[F_{HFP}]_{F\text{-}EA}$ (mol %)[b]	$[F_{HFP}]_{NMR}$ (mol %)	$(R_P)_{av}$ (10^{-2} mol/L·min)	$[M_T]_{out\text{-}av}$ (mol/L)	$(M_n)_{NMR}$ (kDa)	$(M_n)_{GPC}$ (kDa)	PDI	reaction medium
2	59:41	400	24.2 ± 1.36	22.6	1.58	3.28	32.2	29.5	1.5	heterogeneous
13	59:41	310	24.0 ± 1.35	22.5	1.50	3.30	28.9	26.7	1.5	heterogeneous
14	59:41	207	23.5 ± 1.33	22.5	1.18	3.36	24.7	23.7	1.5	heterogeneous
6	66:34	400	26.4 ± 1.42	26.1	1.43	3.31	30.6	29.2	1.5	homogenous (CPP = 352 bar)
15	66:34	310	27.2 ± 1.44	25.4	1.18	3.36	26.2	25.2	1.5	heterogeneous
16	66:34	207	27.2 ± 1.44	25.7	1.14	3.37	25.0	22.7	1.5	heterogeneous
10	73:27	400	31.8 ± 1.58	29.2	1.41	3.32	31.9	29.0	1.5	homogenous (CPP = 291 bar)
17	73:27	310	31.0 ± 1.55	29.1	1.27	3.35	28.5	24.5	1.5	homogenous (CPP = 283 bar)
18	73:27	207	30.8 ± 1.54	29.0	1.02	3.40	24.6	21.5	1.5	heterogeneous

[a] Reaction conditions: $[M_T]_{in} = 3.6$ mol/L; $T = 40$ °C; $\tau = 20$ min; $[I]_{in} = 0.003$ M. For the three feed ratios, the average inlet $scCO_2$ concentration ranges from 74.4 mol % at 400 bar to 71.4 mol % at 207 bar. [b] The error limit in $[F_{HFP}]_{F\text{-}EA}$ corresponds to ±0.3 wt % accuracy and precision error.

fluorine analyses were performed by flask combustion followed by ion chromatography.

Fluorine-19 Nuclear Magnetic Resonance (^{19}F NMR) spectra were recorded on a Bruker Avance spectrometer operating at 470.6 MHz using acetone-d_6 (99.9%) as the solvent and trichlorofluoroethane ($CFCl_3$) as the internal reference. The pulse delay was 5 s, and 256–1024 scans were used.

Differential scanning calorimetry (DSC) measurements were conducted using a TA-Instruments DSC-Q100. The instrument was calibrated using indium. Samples were heated to 150 °C at a heating rate of 10 °C/min. The glass transition temperature was determined from the second heating curve.

Finally, a thermal gravimetric analyzer (TA Instruments TGA-Q500) was used for determining the decomposition temperature (T_d) of the synthesized copolymers. Samples were heated to 800 °C at a heating rate of 10 °C/min in nitrogen. The T_d was determined for 1 wt % polymer loss.

Results and Discussion

Copolymerization Studies. The effect of total inlet monomer concentration ($[M_T]_{in}$) and reaction pressure (P) on the continuous copolymerization of VF2 and HFP was studied. Experiments were carried out at 40 °C in the CSTR using PBP initiator. Three different HFP/VF2 feed ratios were investigated: 59:41, 66:34, and 73:27, giving rise to copolymers containing about 23.3, 26.3, and 30.3 mol % HFP, respectively. The results of these experiments are shown in Tables 1 and 2. The composition, average molecular weight, and molecular weight distribution (MWD) of the copolymers were measured. The molar rate of polymerization (R_P) and the total monomer concentration in the reactor and in the outlet stream ($[M_T]_{out}$) were calculated from the amount of polymer collected (m_p) during the time of steady-state collection (Δt_{ss}), using eqs 1 and 2, respectively. Equations 1 and 2 are based on the assumption that the reactor behaved as an ideal CSTR.

$$R_P = \frac{m_p}{V_R \Delta t_{ss}([F_{HFP}]M_{HFP} + (1 - [F_{HFP}])M_{VF2})} \quad (1)$$

$$[M_T]_{out} = [M_T]_{in} - R_P\tau \quad (2)$$

Here V_R is the reactor volume (100 mL); $[F_{HFP}]$ is the mole fraction of HFP in the copolymer; M_{HFP} and M_{VF2} are the molecular weights of HFP and VF2, respectively; and τ is the average residence time in the reactor.

Both fluorine elemental analysis (F-EA) and ^{19}F NMR were used to determine the copolymer composition. All elemental analyses were on a weight basis with accuracy and precision error limits of ±0.3 wt %. On a mole basis, the error of the elemental analyses depends on the molecular weight of the analyzed element. Since fluorine has the highest molecular weight among the three elements forming the copolymer, only fluorine elemental analysis was considered. Equation 3 was used to calculate $[F_{HFP}]_{F\text{-}EA}$ (mole fraction HFP in the copolymer from F-EA) from the average of two measurements $(W_F)_{av}$ (average weight fraction of fluorine in the copolymer).

$$[F_{HFP}]_{F\text{-}EA} = \frac{19 - 32(W_F)_{av}}{43(W_F)_{av} - 38} \quad (3)$$

A representative ^{19}F NMR spectrum for poly(VF2-*co*-HFP) with high HFP-content is shown in Figure 2 (experiment 6). The detailed chemical shifts are available in the literature.[5,29] The ^{19}F NMR spectrum exhibits various groups of signals; those assigned to VF2 units are centered at −91.4 to −96.2 ppm for

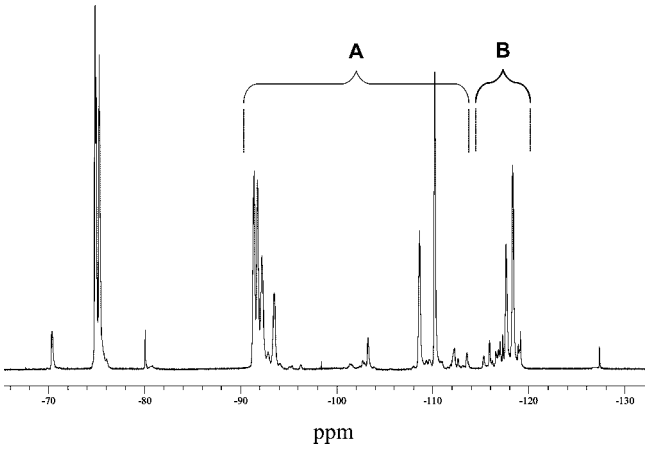

Figure 2. ^{19}F NMR spectrum for copolymer collected in experiment 6 in Table 1 (26.4 ± 1.42 mol % HFP by F-EA, 26.1 mol % HFP by NMR). The resonances due to the CF fluorine in HFP at ca. –181 to –184 ppm are not shown. Copolymer compositions were determined from the integrals of the peaks in the A and B regions.

head-to-tail normal additions ($-CH_2C\mathbf{F}_2CH_2CF-$), at −108.6 to −112.3 ppm for CF_2 groups adjacent to a HFP unit ($-CH_2C\mathbf{F}_2CF_2CF(CF_3)-$), and at −113.6 and −115.9 ppm for the head-to-head reversed addition ($-CH_2C\mathbf{F}_2CF_2CH-$). Those assigned to HFP units are centered at −70.3 and −75 ppm for the pendant CF_3 group ($-CF_2CF(C\mathbf{F}_3)-$), at –115.3 and −117 to −119.2 ppm for CF_2 ($-C\mathbf{F}_2CF(CF_3)-$) group, and at −181.4 and−184.1 ppm for the CF ($-CF_2C\mathbf{F}(CF_3)-$) group. Finally, the peaks at ca. −80 ppm and –126 to –127 ppm are assigned to the $-CF_3$ and $-CF_2$ fluorine in the initiator, respectively.

The mole fraction of HFP monomer in the copolymer ($[F_{HFP}]_{NMR}$) was calculated from eq 4, where *A* corresponds to the sum of the areas of the NMR signals from –91.4 to –115.9 ppm and *B* corresponds to the sum of the areas of the NMR signals from –117 to –119.2 ppm (Figure 2). With the exception of experiment 8, the copolymer composition obtained via fluorine elemental analysis was higher than that from NMR. Nevertheless, the two compositions are close enough to lend confidence to the results.

$$[F_{HFP}]_{NMR} = \frac{B}{A+B} \tag{4}$$

In addition, NMR was used to determine the VF2 reverse defects of chaining (head-to-head VF2 units). Table 3 shows the average VF2 reverse defects (eq 5) for the three current copolymer compositions along with the defects for the 9.2 mol% HFP copolymer previously reported.[16]

$$\text{VF2 reverese defects} = \frac{I_{-113.6} + I_{-115.9}}{A} \tag{5}$$

where $I_{-113.6}$ and $I_{-115.9}$ are the integrals of the signals corresponding to the fluorine of the CF_2 groups at −113.6 and −115.9 ppm, respectively.

Finally, NMR was used to determine the number-average molecular weight (M_n) from end-group analysis of the initiator. End-group analysis can be used to determine M_n to higher values for fluorinated polymers than for hydrocarbon polymers.[16] The number-average molecular weight using the end-group analysis of the PBP initiator by NMR ($(M_n)_{NMR}$) was calculated via eq 6.

$$(M_n)_{NMR} = \frac{(I_{CF2})/2}{(I_{-80ppm}/3)/2}[150[F_{HFP}]_{NMR} + 64(1 - [F_{HFP}]_{NMR})] \tag{6}$$

Here, I_{-80ppm} is the integral of the signal corresponding to the fluorine of the CF_3 group in the C_3F_7 of the PBP initiator located at ca. –80 ppm; I_{CF2} is the sum of the integrals for the signals corresponding to the fluorine in CF_2 groups in the copolymer from –91.4 to –119.2 ppm (a and b in Figure 2).

The main assumption in eq 6 is that termination is by combination, which is consistent with the measured PDI values of around 1.5. This assumption leads to the factor of 1/2 that multiplies ($I_{-80ppm}/3$) in the denominator. Another assumption is that chain transfer reactions to monomers, initiator, and initiator solvent are unimportant. There is no evidence from the literature that chain transfer to VF2 can occur, while chain transfer to HFP, PBP, or Freon 113 are unlikely since these compounds do not contain hydrogen. Finally, chain transfer to polymer that has been reported for VF2-based polymers[2] does not change the average number of initiator end-groups per chain.

Molecular weights determined using both GPC and NMR end-group analysis agree reasonably well. However, the agreement may be somewhat fortuitous since the GPC results are relative to polystyrene standards and in view of the assumptions in the NMR end-group calculation.

Thermal Properties. Table 4 shows the thermal properties of the highest molecular weight copolymer for each of the three copolymer compositions synthesized in this work (experiments 4, 8, and 12 in Table 1). No crystallization or melting was observed for these copolymers. This is consistent with the fact that VF2/HFP copolymers become completely amorphous for an HFP content higher than 19–20 mol %.[2,3] From Table 4, the increase of the $-CF_3$ side group with increasing HFP content in the copolymer raised the glass transition temperature (T_g). This increase of T_g with increasing HFP-content is consistent with the T_g of PVDF homopolymer (typical T_g for PVDF = −40 °C[30]) and that of ca. 9.2% HFP poly(VF2-*co*-HFP) (−31.4 °C[16]).

Effect of Total Monomer Concentration. For each HFP/VF2 feed ratio, four experiments were carried out with $[M_T]_{in}$ varying from 1.5 to 6.5 mol/L, at otherwise identical conditions. The results are given in Table 1 and Figures 3a−d, 4a−d, and 5a−d for the 59:41, 66:34, and 73:27 HFP/VF2 feed ratios, respectively. In a CSTR, the concentration that affects the polymerization is the concentration inside the reactor, which is the same as the effluent concentration ($[M_T]_{out}$). Consequently, the results in these figures are plotted versus the average $[M_T]_{out}$ from F-EA and NMR ($[M_T]_{out\text{-}av}$). All experiments were run at the same temperature, average residence time (τ) and feed initiator concentration ($[I]_{in}$). Therefore, the initiator concentration in the CSTR and in the effluent ($[I]_{out}$) should be the same for each of these experiments (eq 7).

$$[I]_{out} = \frac{[I]_{in}}{1 + k_d\tau} \tag{7}$$

where k_d is decomposition rate constant of the initiator.

Plots a and b in Figures 3, 4, and 5 show the effect of $[M_T]_{out}$ on R_P and $(M_n)_{GPC}$, respectively. For all three monomer feed ratios, both R_P and M_n increase with $[M_T]_{out}$ in a linear manner. The dotted lines in plots a and b represent the best fit of the experimental data by a straight line passing through the origin. The fit is excellent, with a coefficient of determination (R^2) near unity for all three feed ratios. The first-order dependence of R_P and M_n on the monomer concentration is characteristic of a conventional solution polymerization. This is expected for the 73:27 HFP/VF2 feed ratio since all of these polymerizations were homogeneous. However, for the 66:34 and 59:41 feed ratios, some of the polymerizations were homogeneous while others were heterogeneous, i.e., the polymer precipitated in the reactor. In particular, the low-molecular-weight copolymers, formed at low inlet monomer concentrations, were soluble while the high-molecular-weight polymers precipitated during the

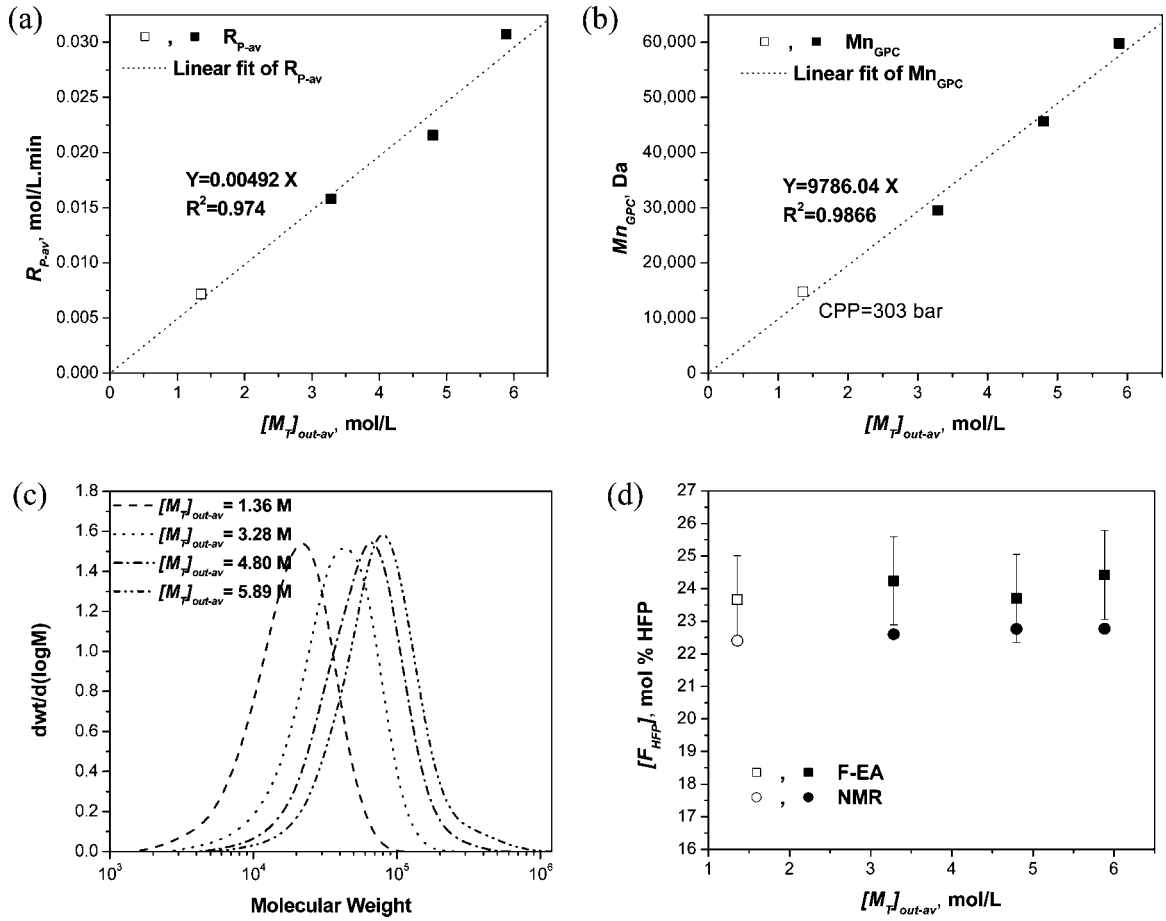

Figure 3. Effect of total monomer concentration for HFP/VF2 feed ratio of 59:41 on (a) R_P; (b) M_n; (c) MWDs; (d) $[F_{HFP}]$. In (a), (b), and (d), the filled symbols are for heterogeneous polymerizations while the open ones are for homogeneous polymerizations. In (b), CPP is the cloud-point pressure. Reaction conditions are given in Table 1.

Table 3. Average VF2 Reverse Defects for poly(VF2-*co*-HFP) Polymers Synthesized in $scCO_2$[a]

copolymer	average VF2 reverse defects, %
poly(VF2-*co*-9.2 mol% HFP)[16]	6.1
poly(VF2-*co*-23.3 mol% HFP)	3.1
poly(VF2-*co*-26.3 mol% HFP)	2.6
poly(VF2-*co*-30.3 mol% HFP)	2.4

[a] Reaction conditions: $T = 40$ °C; $P = 400$ bar.

Table 4. Thermal Properties of poly(VF2-*co*-HFP)

experiment in Table 1	4	8	12
% mol HFP in copolymer[c]	24.4	26.2	30.8
T_g[a] (°C)	−20.8	−18.4	−15.6
T_d[b] (°C)	347	377	374

[a] Glass transition temperature. [b] 1 wt % decomposition temperature in nitrogen. [c] From fluorine elemental analysis.

polymerization. Nevertheless, for these two feed ratios, all of the data points fell on the same straight line, suggesting that precipitation does not influence R_P and M_n. The same linear dependence was reported previously for the copolymerization of a semicrystalline composition of poly(VF2-*co*-HFP) (with ca. 9.2 mol % HFP) in $scCO_2$.[16] The copolymerization of these fluoropolymers appears to occur mainly in the CO_2-rich fluid phase. If there had been a significant amount of polymerization in the precipitated polymer phase, a higher order of dependence of both R_p and M_n on total monomer concentration would have been observed,[22,23] especially for higher molecular weights. For example, in the polymerization of poly(acrylic acid) in $scCO_2$ where the polymer phase was believed to be the main locus of polymerization,[23] the order with respect to $[M_T]_{out}$ was significantly greater than unity for both R_P and the viscosity-average molecular weight.[22]

Plot c in Figures 3, 4, and 5 shows the MWDs of the synthesized copolymers for the three feed ratios. With one exception, the MWDs are unimodal with a polydispersity index (PDI) of 1.5. The exception is for the 59:41 feed ratio, where a slight tail developed for the highest monomer concentration ($[M_T]_{in} = 6.5$ mol/L, $[M_T]_{out-av} = 5.89$ mol/L, experiment 4 in Table 1). Figure 6 shows the MWDs of the three current copolymers compared with the MWD of the copolymer produced with a 26.5:73.5 HFP/VF2 feed ratio (9.2 mol % HFP in the copolymer),[16] for $[M_T]_{in} = 6.5$ mol/L. The MWD of the 26.5:73.5 feed ratio copolymer has a long tail and a broad shoulder. Increasing the HFP/VF2 feed ratio to 59:41 (23.3 mol % HFP in the copolymer) diminished the tail, while further increase of the HFP content of the copolymer eliminated the tail completely for the 66:34 and 73:27 feed ratios (26.3 and 30.3 mol % HFP in the copolymer, respectively). Clearly, the bimodality/tail decreases with HFP content in the copolymer. For comparison, the MWDs of PVDF homopolymer synthesized in $scCO_2$ showed bimodal MWDs and much higher PDIs at lower monomer concentrations.[20]

In the case of PVDF polymerization, bimodality has been the subject of some controversy. It has been attributed either to a simultaneous polymerization in both the fluid and the polymer phases, taking into account the transport of polymeric radicals between the two phases,[31] or to a homogeneous polymerization, recognizing the transition of the termination reaction from a kinetically controlled regime to a diffusion-controlled regime

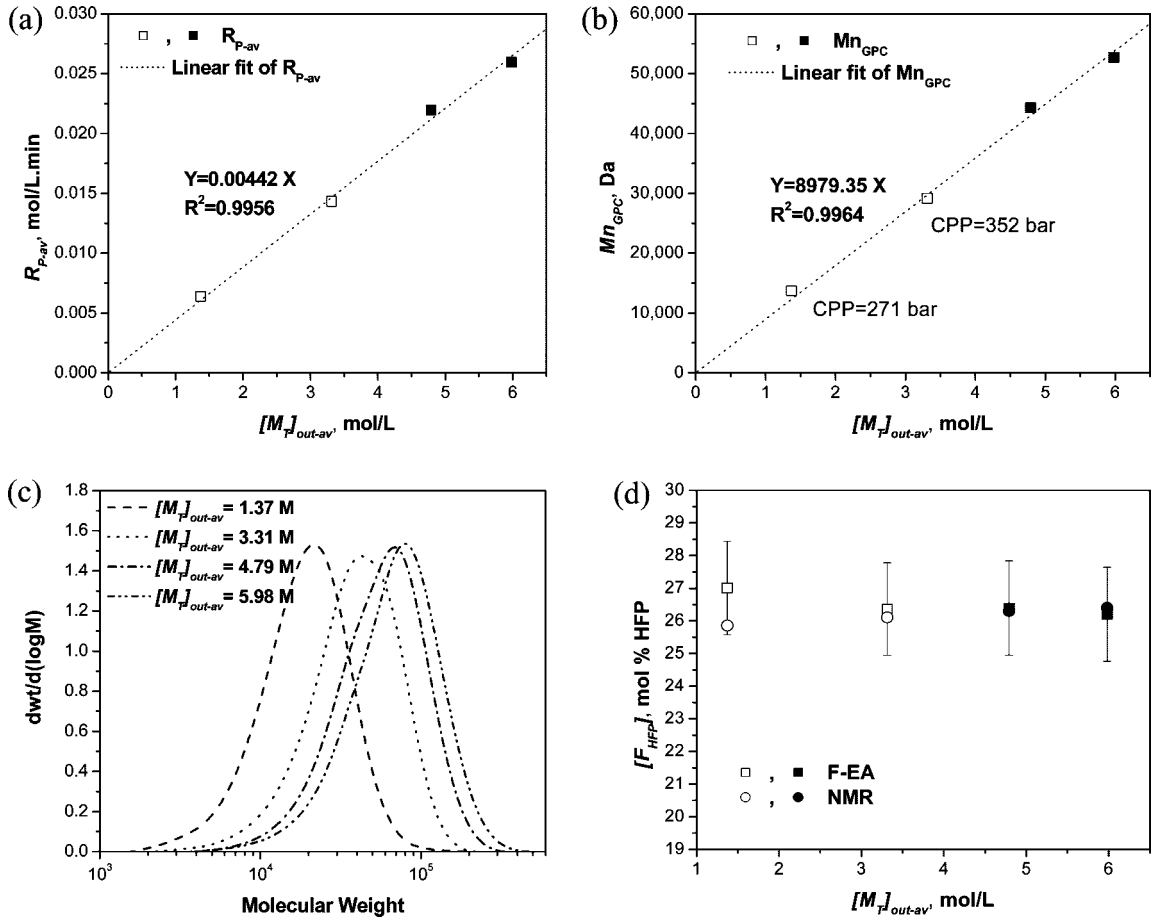

Figure 4. Effect of total monomer concentration for HFP/VF2 feed ratio of 66:34 on (a) R_P; (b) M_n; (c) MWDs; (d) $[F_{HFP}]$. In (a), (b), and (d), the filled symbols are for heterogeneous polymerizations while the open ones are for homogeneous polymerizations. In (b), CPP is the cloud-point pressure. Reaction conditions are given in Table 1.

with increasing macroradical molecular weight.[32] In our recent contribution on the continuous precipitation polymerization of low-HFP-content poly(VF2-*co*-HFP),[16] it was concluded that the CO_2-rich continuous phase is the main locus of polymerization. Moreover, the heterogeneous polymerization model could not account for the change in the MWD tail with polymerization conditions in case of poly(VF2-*co*-HFP).[16] On the other hand, the homogeneous polymerization model could explain successfully the change in the MWD tail. In the current work, the independence of R_P and M_n of the mode of polymerization, i.e., precipitation versus solution, supports the contention that the CO_2-rich continuous phase is the main locus of polymerization. For this situation, the decrease of the MWD tail/bimodality with HFP content in the copolymer can be explained as follows. First, chains with HFP terminal groups cannot terminate with similar HFP-ended chains because of the very low reactivity of the terminal HFP unit.[5,6] Therefore, the probability of the kinetically controlled termination decreases as the HFP concentration is increased. As a result, the chain length, at which the termination reaction shifts from kinetic control to macroradical diffusion control, increases as the HFP concentration increases. In the homogeneous model, the MWD tail results from chains whose termination is diffusion-limited.[32] Therefore, the tail should decrease as HFP concentration increases. Second, the increase of HFP content in the copolymer increases the molecular weight of the average monomer unit. Consequently, the molecular weight at which the transition between the two termination regimes occurs shifts to a higher molecular weight even for the same chain length. This leads to a decrease in the MWD tail. Finally, the decrease of both the backbone hydrogen and the VF2 reverse defects (Table 3) with the increase of HFP-content in the copolymer reduces the probability of chain transfer to polymer. Chain transfer to polymer coupled with termination by combination is responsible for very high-molecular-weight chains. Accordingly, the population of high-molecular-weight chains, which constitute the tail, decreases with the increase of HFP content in the copolymer.

Finally, plot d in Figures 3, 4, and 5 shows the effect of total monomer concentration on HFP incorporation into the copolymer. For each feed ratio, the copolymer composition does not vary significantly with monomer concentration. Even though the copolymer precipitated during the experiments with high monomer concentrations for the 59:41 and 66:34 feed ratios, the precipitation did not affect the copolymer composition. In comparison, at a much lower feed ratio of 27:73 (ca. 9.2 mol % HFP in copolymer),[16] HFP incorporation into the copolymer decreased slightly with increasing total monomer concentration. This was attributed to preferential partitioning of HFP into the precipitated copolymer particles.[16] For the high-HFP-content amorphous copolymers, no preferential partitioning is apparent. This can be explained in two ways. First, solubility of the copolymer in $scCO_2$ increases with HFP content,[33] causing the fraction of precipitated chains to decrease. This makes any partitioning less observable. The second possibility is that since $scCO_2$ becomes a better solvent for chains with higher HFP content,[33] such precipitated chains become more expanded in $scCO_2$. Consequently, preferential partitioning should be reduced since the composition of the two phases becomes increasingly similar.

Effect of Reaction Pressure. The effect of pressure was evaluated from 207 to 400 bar at otherwise identical conditions.

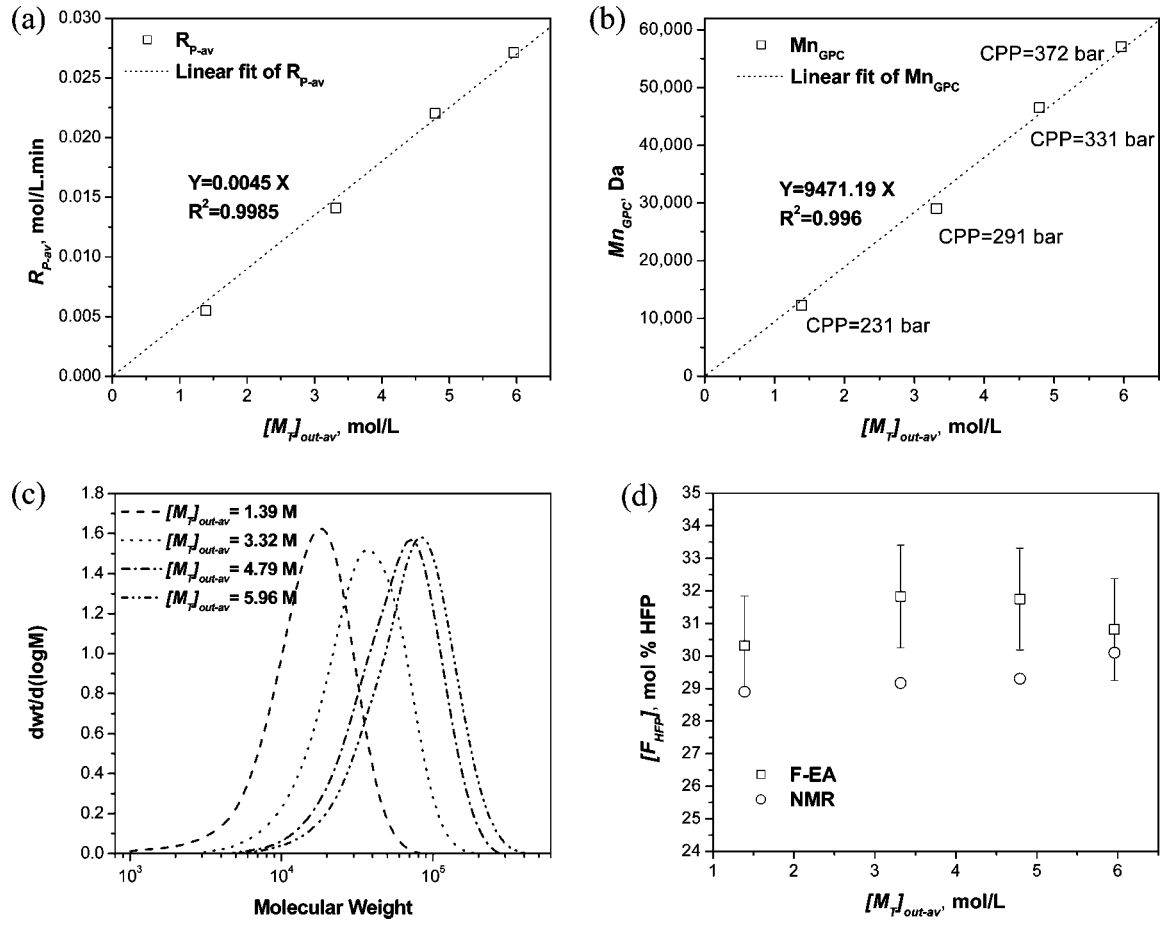

Figure 5. Effect of total monomer concentration for HFP/VF2 feed ratio of 73:37 on (a) R_P; (b) M_n; (c) MWDs; (d) [F_{HFP}]. In (b), CPP is the cloud-point pressure. Reaction conditions are given in Table 1.

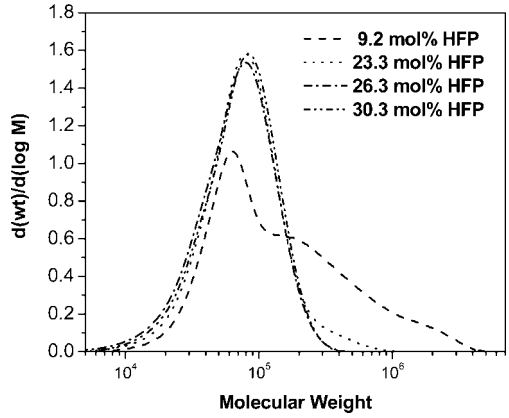

Figure 6. MWDs of poly(HFP-*co*-VF2) synthesized in $scCO_2$ for $[M_T]_{in}$ = 6.5mol/L, P = 400 bar, T = 40 °C, τ = 20 min, $[I]_{in}$ = 3 mM.

The results are given in Table 2 and Figures 7a−d, 8a−d, and 9a−d for the 59:41, 66:34, and 73:27 HFP/VF2 feed ratios, respectively.

Plots a and b in Figures 7, 8, and 9 show the effect of pressure on the R_P and M_n for the three feed ratios. The increase of pressure from 207 to 400 bar resulted in a 20–30% increase in both R_P and M_n. For comparison, in case of the semicrystalline low-HFP copolymers, the effect was more pronounced with about an 80% increase for the same range of pressure.[16]

For classical solution polymerization, eqs 8 and 9 describe the rate of polymerization and the number-average molecular weight, respectively. For a copolymerization at constant temperature and pressure, the copolymerization propagation rate constant (k_p) is a function of the mole fractions of the monomers, and their reactivity ratios. Equation 10 shows the expression for k_p in the case of the terminal model.[34] The termination rate is usually diffusion-controlled.[34,35] For a copolymerization, the simplest "ideal diffusion" model for the copolymerization termination rate constant (k_t) is a linear combination of the termination rate constants for the two homopolymerizations (eq 11).[36]

$$R_P = k_p\left(\frac{2fk_d}{k_t}\right)^{0.5}[M][I]^{0.5} \tag{8}$$

$$M_n = \alpha M_o k_p (2fk_d k_t)^{-0.5}[M][I]^{-0.5} \tag{9}$$

$$k_p = \frac{r_1 f_1 + 2f_1 f_2 + r_2 f_2}{(r_1 f_1/k_{11}) + (r_2 f_2/k_{22})} \tag{10}$$

$$k_t = F_1 k_{t1} + F_2 k_{t2} \tag{11}$$

In these equations, f is the initiator decomposition efficiency; $[M]$ and $[I]$ are the concentrations of monomer(s) and initiator in the reactor; f_i, F_i,r_i, k_{ii}, and k_{ti} are the mole fraction in the feed, mole fraction in the copolymer, reactivity ratio, self-propagation rate constant, and self-termination rate constant for monomer i, respectively. The value of α is 1 for termination by disproportionation and 2 for termination by combination; M_o is the average molecular weight of a monomer unit in the polymer.

From transition state theory, the effect of pressure on a rate constant is given by eq 12. If the activation volume is constant

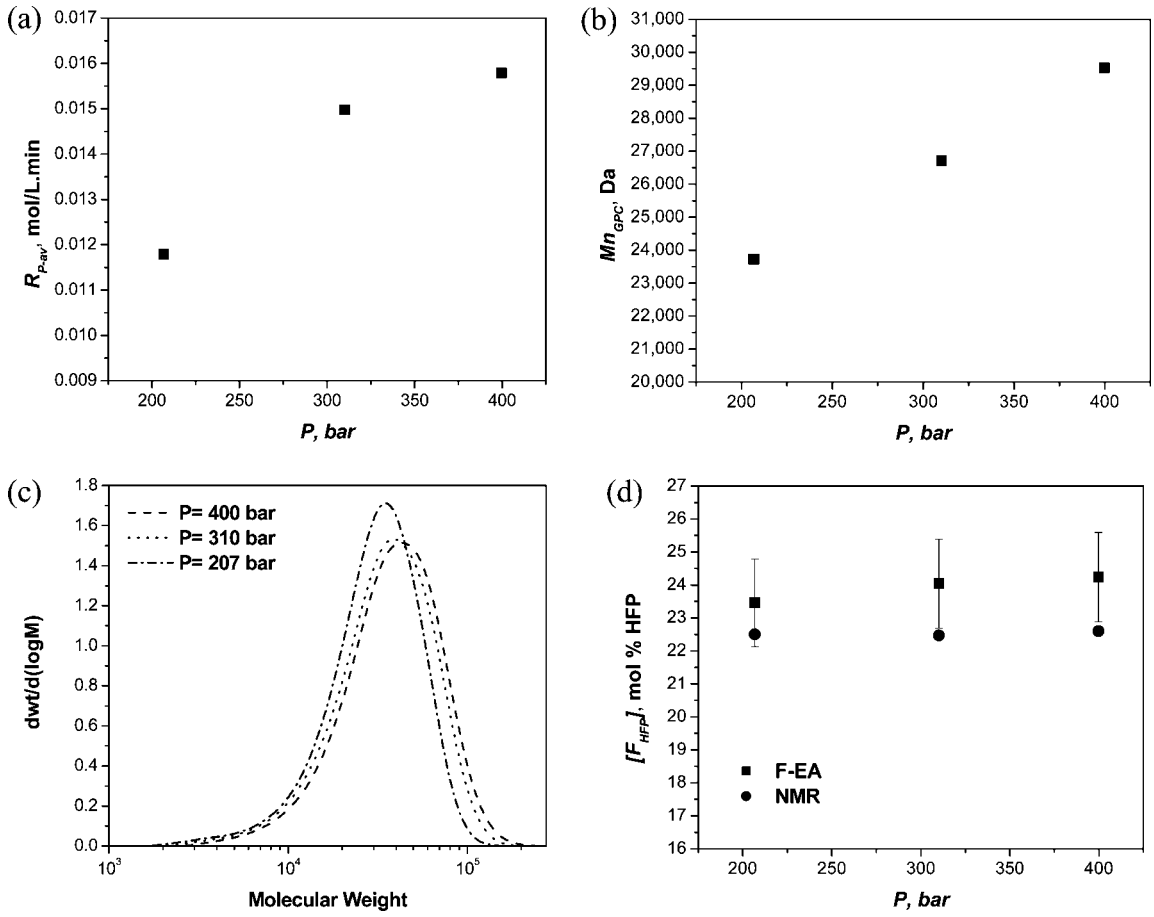

Figure 7. Effect of reaction pressure for HFP/VF2 feed ratio of 59:41 on (a) R_P; (b) M_n; (c) MWDs; (d) $[F_{HFP}]$. Reaction conditions are in Table 2.

over the pressure range under consideration, eq 12 can be integrated to give eq 13.

$$\frac{\mathrm{d}\ln k}{\mathrm{d}P} = -\frac{\Delta V^*}{RT} \tag{12}$$

$$k_2 = k_1 \times \exp\left(-\frac{\Delta V^*}{RT}(P_2 - P_1)\right) \tag{13}$$

where ΔV^* is the activation volume, R is the universal gas constant, T is the temperature, and k_1 and k_2 are the rate constants at pressures P_1 and P_2, respectively.

From the 73:27 feed ratio results, experiments 17 and 18 (Table 2) are for homogeneous solution polymerizations at 400 and 310 bar, respectively. Hence, the results of these two experiments can be used to estimate a value for the overall activation volume of polymerization. Using eq 8 and neglecting the effect of pressure on f and k_d for PBP,[18] $K_{\text{Poly-400-bar}}/K_{\text{Poly-310-bar}} = 1.12$, where $K_{\text{Poly}} = k_p k_d^{0.5}/k_t^{0.5}$. Substituting this value into eq 13 gives an overall activation volume of polymerization of –0.033 L/mol. This activation volume accounts for about a 28% increase in K_{Poly} over the pressure range from 207 to 400 bar. Using the same procedure, eq 9 results in a value of −0.035 L/mol for the activation volume of $K_{\text{Mwt}} = k_p/(k_d k_t)^{0.5}$, which predicts about a 30% increase in M_n for the same pressure range. Therefore, the observed increases in R_P and M_n with pressure for the high-HFP-content copolymers can be accounted for by the effect of pressure on the reaction rate constants. This contrasts with the low-HFP-content copolymers, where this effect was not sufficient.[16]

The estimated values for the activation volumes for K_{Poly} and K_{Mwt} lie within the relatively broad reported range in the literature.[34,37] By solving eqs 14 and 15 simultaneously, values of $\Delta V^*_d = +0.002$ L/mol and $(\Delta V^*_p - 1/2\Delta V^*_t) = -0.034$ L/mol are obtained. The low positive value of ΔV^*_d agrees with the low values of the activation volumes reported for thermal decomposition.[34,37] In addition, the low value of ΔV^*_d is consistent with the near-nil pressure dependence of the decomposition kinetics of other initiators in $scCO_2$.[18] Similarly, the value obtained for $(\Delta V^*_p - 1/2\Delta V^*_t)$ is very close to the value obtained using the individual values of ΔV^*_p and ΔV^*_t proposed by Morbidelli et al.[31] for VF2 polymerization, based on typical values for vinyl monomers ($\Delta V^*_p = -0.025$ L/mol and $\Delta V^*_t = +19$ L/mol).

$$\Delta V^*_{\text{Poly}} = \left(\Delta V^*_p - \frac{1}{2}\Delta V^*_t\right) + \frac{1}{2}\Delta V^*_d \tag{14}$$

$$\Delta V^*_{\text{Mwt}} = \left(\Delta V^*_p - \frac{1}{2}\Delta V^*_t\right) - \frac{1}{2}\Delta V^*_d \tag{15}$$

where ΔV^*_p, ΔV^*_t, and ΔV^*_d are the activation volumes for the propagation, termination, and initiator decomposition reactions, respectively.

Finally, plots c and d in Figures 7, 8, and 9 show the effect of pressure on the MWDs and HFP incorporation in the copolymer. All the MWDs are perfectly unimodal. For each feed ratio, the copolymer composition is essentially constant. Similar to the effect of monomer concentration, no selective monomer partitioning is observed with increasing pressure, i.e., with increasing copolymer fraction in the reactor. Again, this is different from the case of the low-HFP-content copolymers[16].

Copolymerization Reaction Constants. Whether the copolymer precipitated or not, R_P and M_n were linear with $[M_T]_{\text{out}}$ for all the three feed compositions. Consequently, eqs 8 and 9 can be used to estimate the copolymerization rate constants.

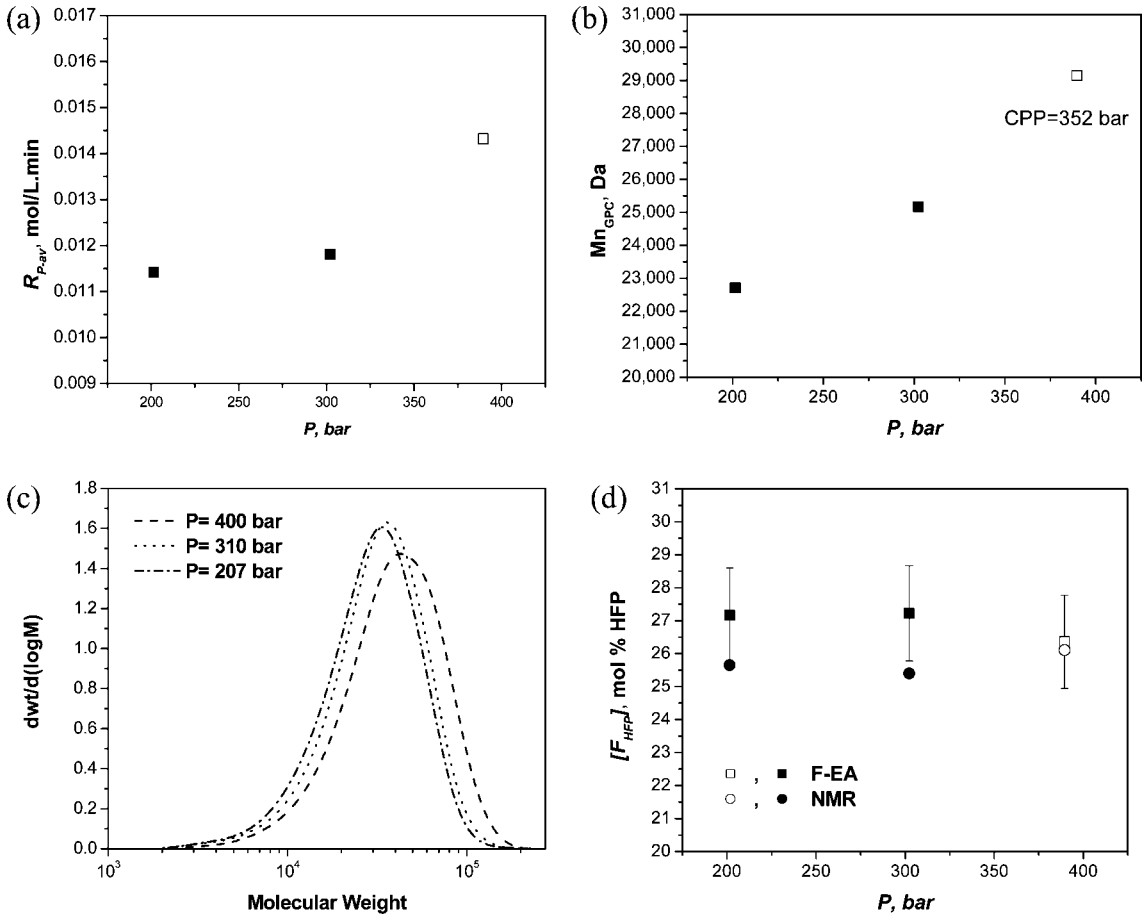

Figure 8. Effect of reaction pressure for HFP/VF2 feed ratio of 66:34 on (a) R_P; (b) M_n; (c) MWDs; (d) $[F_{HFP}]$. In (a), (b), and (d), the filled symbols are for heterogeneous polymerizations while the open ones are for homogeneous polymerizations. In (b), CPP is the cloud-point pressure. Reaction conditions are in Table 2.

By fitting the experimental results to eqs 8 and 9 after setting $[M] = [M_T]_{out}$ and $[I] = [I]_{out}$, and combining them with eq 7, values of $k_p/k_t^{0.5}$ for the copolymerization of VF2 with HFP and k_d for PBP decomposition in $scCO_2$ can be estimated as shown in eqs 16 and 17, respectively.

$$\frac{k_p}{k_t} = \left(\frac{S_{R_p} \times S_{M_n}}{\alpha M_o}\right)^{0.5} \tag{16}$$

$$k_d = \frac{\alpha M_o}{2f[I_{in}]\left(\frac{S_{M_n}}{S_{R_p}}\right) - \tau\alpha M_o} \tag{17}$$

Here, S_{R_p} and S_{M_n} are slopes of the best straight line passing through the origin for each set of experimental data of R_p and M_n versus $[M_T]_{out}$, respectively.

There is no evidence in the literature for termination by disproportionation,[20] and in view of the measured PDI values of around 1.5, termination by combination was assumed and a value of $\alpha = 2$ was used. A value of $f = 0.6$ was assumed, similar to that observed for diethyl peroxydicarbonate decomposition in $scCO_2$.[18] Values of M_o of 84.06, 86.65, and 90.08 were used for the 59:41, 66:34, and 73:27 feed ratios, respectively. These M_o values were calculated from the average of the copolymer compositions from F-EA and NMR (Table 1), for each feed ratio. Only the molecular weight data from GPC were used to obtain S_{M_n}. However, as shown in Tables 1 and 2, the differences between molecular weights from GPC and NMR end-group analysis are small.

The results of this analysis are presented in Table 5 and Figure 10. For comparison, the values reported recently[16] for PVDF and the low-HFP-content copolymer made by continuous copolymerization (HFP/VF2 feed ratio of 26.5:73.5; average copolymer composition of 9.2 mol % HFP) are included. The values of $k_p/k_t^{0.5}$ in Figure 10 are plotted versus HFP mol % in the effluent monomer (eq 18) since this is the actual concentration inside the CSTR.

$$(f_{HFP})_{out} = \frac{(f_{HFP})_{in}[M_T]_{in} - \tau F_{HFP}(R_p)_{av}}{[M_T]_{out-av}} \tag{18}$$

where $(f_{HFP})_{in}$ and $(f_{HFP})_{out}$ are the mole fraction of HFP in the feed and effluent monomers, repectively, and F_{HFP} is the mole fraction of HFP in the copolymer, based on the average from NMR and F-EA.

For low HFP/VF2 ratios, $k_p/k_t^{0.5}$ decreases significantly with increasing HFP mole fraction, while the decrease is much less for higher ratios. Since HFP has an essentially zero reactivity ratio,[4–6,33] HFP monomer units cannot add to growing chains with a terminal HFP unit. Therefore, k_p is expected to decrease with increasing HFP/VF2 ratio since the polymeric radicals with terminal HFP units are much less reactive than those with terminal VF2 units. For the same reason, the intrinsic termination rate constant should also decrease with increasing HFP mole fraction. However, since termination is diffusion-controlled,[34,35] at least for the high-molecular-weight chains, the effect of HFP concentration on the observed termination rate constant is weaker. In addition, $k_p/k_t^{0.5}$ is more sensitive to changes in k_p than in k_t. Thus, the large observed decrease of $k_p/k_t^{0.5}$, especially at low HFP concentrations, is reasonable. Moreover, the increase of HFP content in the polymeric chains increases their solubility in $scCO_2$.[33] This results in an increase of the viscosity of the

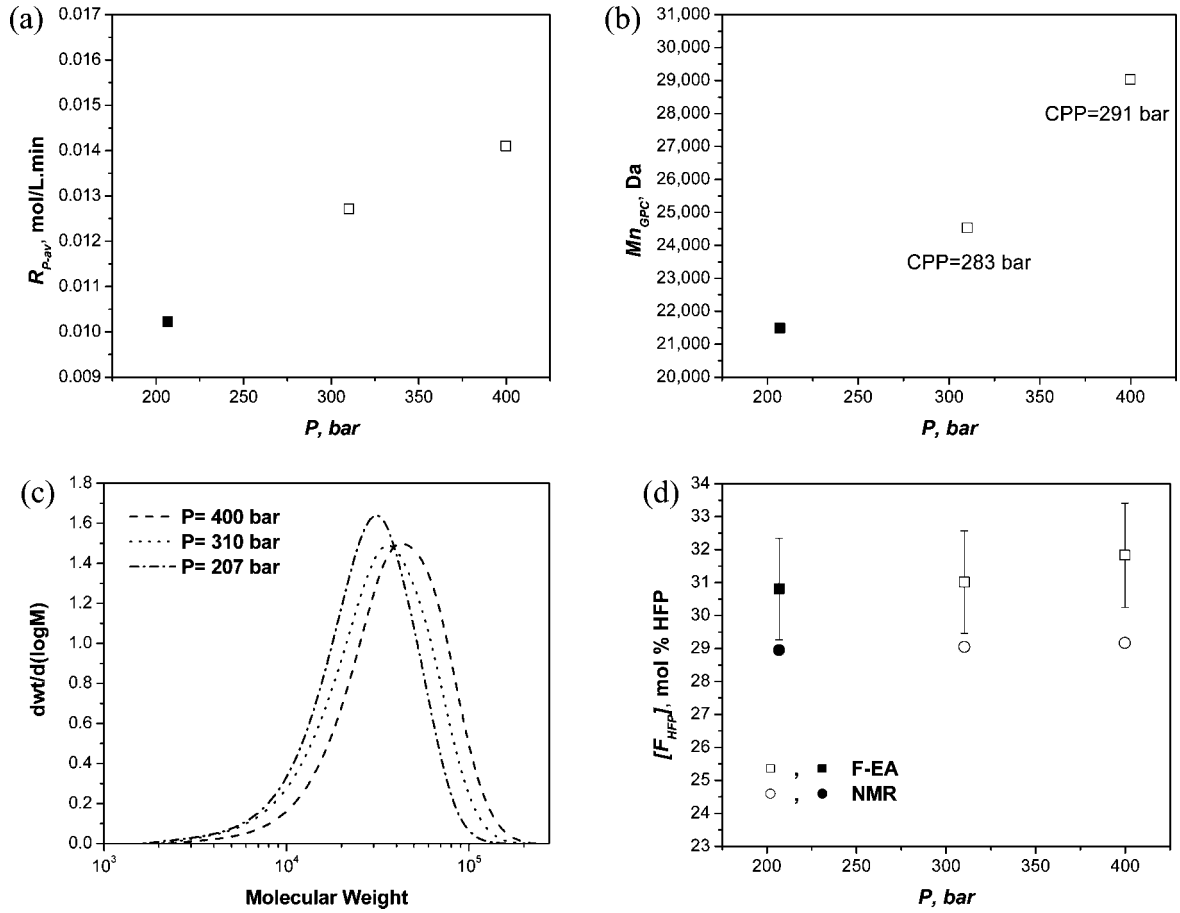

Figure 9. Effect of reaction pressure for HFP/VF2 feed ratio of 73:27 on (a) R_P; (b) M_n; (c) MWDs; (d) $[F_{HFP}]$. In (a), (b), and (d), the filled symbols are for heterogeneous polymerizations while the open ones are for homogeneous polymerizations. In (b), CPP is the cloud-point pressure. Reaction conditions are in Table 2.

Table 5. Values for $k_p/k_t^{0.5}$ for poly(VF2-*co*-HFP) and PVDF and k_d of the PBP Initiator[a]

	HFP/VF2 mol feed ratio	average HFP/VF2 mole effluent ratio	$k_p/k_t^{0.5}$ ($L^{0.5}/mol^{0.5}\cdot s^{0.5}$)	k_d (10^{-4} s^{-1})
PVDF[16]	0	0	1.3	–
poly(VF2-*co*-9.2 mol % HFP)[16]	26.5:73.5	28.2:71.8	0.68	4.01
poly(VF2-*co*-23.3 mol % HFP)	59:41	62.5:37.5	0.54	7.38
poly(VF2-*co*-26.3 mol % HFP)	66:34	69.6:30.4	0.48	7.51
poly(VF2-*co*-30.3 mol % HFP)	73:27	76.7:23.3	0.49	7.55

[a] $P = 400$ bar and $T = 40$ °C.

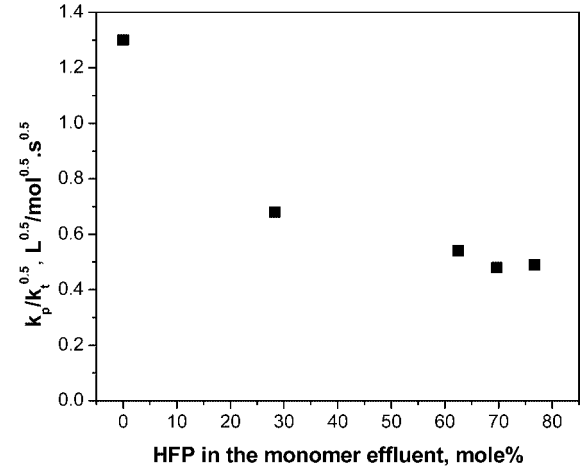

Figure 10. Effect of HFP on $k_p/k_t^{0.5}$ in $scCO_2$ at 400 bar and 40 °C.

reaction mixture, which decreases the observed termination rate constant. Hence, the rate of decrease of the $k_p/k_t^{0.5}$ ratio decreases with increasing HFP content.

Equation 17 was used to estimate the decomposition rate constant of PBP (k_d) in the reaction mixture for each of the three feed ratios in this work (Table 5). In addition, the value of k_d that we reported recently in the continuous polymerization of semicrystalline, low-HFP copolymer is included for comparison. The difference in the values of k_d estimated from the low- and high-HFP copolymerization data may be the result of neglecting the possibility of initiator partitioning between the fluid phase and the polymer phase in case of the low-HFP-content copolymer. This assumption is implicit when the feed initiator concentration $[I_{in}]$ is used to calculate the concentration of the initiator in the CSTR $[I_{out}]$ from eq 7. Since all the experiments for the 73:27 HFP/VF2 feed ratio were homogeneous, the value of $k_d = 7.55 \times 10^{-4}$ s^{-1} is free of this assumption and represents the actual decomposition constant of PBP in the reaction medium at 400 bar and 40 °C. This value of k_d was used in eq 17 to calculate a value of $[I_{in}]$ for each feed composition. The resulting values were 2.99, 2.97, and 2.05 mmol/L for the 66:34, 59:41, and 73:27 monomer feed ratios, respectively. Compared to the actual initiator feed concentration of 3 mmol/L, these values suggest that the partitioning of the initiator into the polymer phase is near nil for the high-HFP-content amorphous copolymers, while appreciable for the low-HFP semicrystalline ones. This can be rationalized in two ways.

Table 6. Reactivity Ratio Pairs for the Copolymerization of VF2 with HFP

set	r_{HFP}	r_{VF2}	reference
A[a,d]	0[a]	6.7	Moggi et al.[39]
B[a,d]	0	5	Logothetis et al.[40]
C[a,e]	0	2.45	Bonardelli et al.[41]
D[a,f]	0.12 ± 0.05	2.9 ± 0.6	Gelin et al.[38]
E[a,g]	0	5.13 ± 0.44	Tai et al.[42]
F[h]	0	3.6[a]	Beginn et al.[43]
	0[b]	8.2[b]	
	0[c]	4.8[c]	
G[I]	0 ± 0.08[c]	3.61 ± 0.71[c]	Ahmed et al.[33]
	0.09 ± 0.09[c]	4.67 ± 0.77[c]	
H[j]	0	3.2[c]	Ahmed et al.[16]

[a] Based on copolymer composition obtained from NMR. [b] Based on copolymer composition obtained from F-EA. [c] Based on copolymer composition obtained from the average of both NMR and F-EA. [d] Batch emulsion polymerization at 70–130 °C and 20–70 bar (exact conditions not known). [e] Batch emulsion polymerization at 85 °C and 13.2 bar, values from NMR. [f] Batch solution polymerization in acetonitrile at 120 °C. [g] Batch precipitation polymerization in $scCO_2$ at 55 °C and initial pressure of 276 bar. [h] Batch polymerization in $scCO_2$ at 50 °C and initial pressure of 280 bar. [I] Batch polymerization in $scCO_2$ at 35 °C and initial pressure of 310 and 415 bar. [j] Continuous precipitation polymerization of low HFP content in $scCO_2$ at 40 °C and reaction pressure of 400 bar.

First, the decrease in the fraction of precipitated chains due to the increase of polymer solubility with HFP content. Second, the increase in the expansion of the precipitated chains with the increase of their HFP-content as a result of $scCO_2$ becoming a better solvent for such chains. This increase should reduce the preferential partitioning of the initiator between the two phases since the difference in composition between the two phases becomes less pronounced.

Reactivity ratios. Table 6 shows the reactivity ratios reported in the literature for VF2/HFP free-radical copolymerizations. Most of the reported values of HFP (r_{HFP}) are zero or very close to zero. However, there is a substantial difference in the reported values for the reactivity ratio of VF2 (r_{VF2}). This is probably due to differences from study to study in (a) the mode of polymerization (emulsion, precipitation, solution, etc.) (b) reaction conditions, and/or (c) monomer composition drift for batch reactors. Additional differences can arise from the different analytical methods used for determining the copolymer composition. Most of the reported values are for copolymer compositions determined from NMR; only a few are from F-EA. Moreover, due to the heterogeneity of the polymerization systems, most of the reported values contain a "concentration factor" that changes with reaction conditions. Therefore, the reported values should be considered as "effective" reactivity ratios. The only exception is the reactivity ratios for VF2/HFP solution copolymerization in acetonitrile reported by Gelin et al. at 120 °C.[38]

The Mayo−Lewis equation[44] (eq 19) was used to calculate the reactivity ratios of HFP and VF2 from the present results. These ratios were estimated by fitting eq 19 to the experimental data using nonlinear regression (DataFit with the Levenberg–Marquardt algorithm[45]). The HFP mole fraction in the effluent monomer was calculated from eq 18; the HFP mole fraction in the copolymer was the average of the values from F-EA and NMR. The calculation was based on the three compositions covered in this work plus a fourth composition from our recent report of low-HFP-content copolymerization.[16] Only the data for three homogeneous experiments for the three feed ratios in the current work (experiments 1, 5, and 9 from Table 1) plus the data for experiment 1 in Table 1 from our recent report[16] were used. This last experiment was chosen since it is expected to have the least partitioning of the monomers.[16] The values of the reactivity ratios obtained with the 95% confidence limits are $r_{HFP} = 0 \pm 0.05$ and $r_{VF2} = 3.3 \pm 0.74$ at 40 °C and 400 bar.

$$F_{HFP} = \frac{r_{HFP}(f_{HFP})_{out} + (f_{HFP})_{out}(1 - (f_{HFP})_{out})}{r_{HFP}(f_{HFP})_{out} + 2(f_{HFP})_{out}(1 - (f_{HFP})_{out}) + r_{VF2}(1 - (f_{HFP})_{out})^2} \quad (19)$$

where $(f_{HFP})_{in}$ is the mole fraction of HFP in the feed monomers to the reactor and F_{HFP} is the mole fraction of HFP in the copolymer, based on the average from NMR and F-EA.

Conclusions

The continuous copolymerization of VF2 with HFP in $scCO_2$ was successfully carried out in a CSTR for three HFP/VF2 molar feed ratios: 59:41, 66:34, and 73:27. The effects of total monomer concentration and reaction pressure were both explored at otherwise constant conditions.

Both R_p and M_n increased linearly with total monomer concentration, and both increased with pressure by about 20–30% from 207 to 400 bar at all three HFP/VF2 feed ratios. This latter increase was accounted for by the effect of pressure on the reaction rate constants. All of the MWDs were perfectly unimodal with a PDI of 1.5 except for the highest monomer concentration at the 59:41 feed ratio, in which a small tail appeared. A comparison with PVDF and low-HFP-content poly(VF2-*co*-HFP) suggests that the bimodality/tail/PDI decreases with HFP content in the copolymer.

The $k_p/k_t^{0.5}$ ratio for the copolymerization decreased with increasing HFP content in the copolymer. However, its rate of change also decreased with increasing HFP content. The decrease of $k_p/k_t^{0.5}$ with increasing HFP was attributed to the low reactivity of HFP-terminated polymer radicals, while the increase of the viscosity of the reaction medium with increasing solubility of the high-HFP-content copolymers could account for the decreased rate of change of $k_p/k_t^{0.5}$ with HFP content.

The value of k_d of PBP at 40 °C in the reaction mixture was calculated from the homogeneous copolymerizations of the 73:27 feed ratio. Comparison with the values obtained from the copolymerizations at the other feed ratios suggests that PBP has an appreciable solubility in the semicrystalline, low-HFP-content polymer phase but negligible solubility in the high-HFP-content amorphous copolymers.

Acknowledgement. This material is based upon work supported by the STC Program of the National Science Foundation under Agreement No. CHE-9876674.

References and Notes

(1) Dixon, S.; Rexford, D. R.; Rugg, J. S. *Ind. Eng. Chem.* **1957**, *49* (10), 1687–1690.
(2) Apostolo, M.; Arcella, V.; Storti, G.; Morbidelli, M. *Macromolecules* **1999**, *32* (4), 989–1003.
(3) Ajroldi, G.; Pianca, M.; Fumagalli, M.; Moggi, G. *Polymer* **1989**, *30* (12), 2180–2187.
(4) Ferguson, R. C. *J. Am. Chem. Soc.* **1960**, *82* (10), 2416–2418.
(5) Pianca, M.; Bonardelli, P.; Tato, M.; Cirillo, G.; Moggi, G. *Polymer* **1987**, *28* (2), 224–230.
(6) Schmiegel, W. W. *Angew. Makromol. Chem.* **1979**, *76–7*, 39–65.
(7) Office for Official Publications of the European Communities. Document no. 302M2690-Solvay/Montedison−Ausimont Merger Procedure. (http://ec.europa.eu/comm/competition/mergers/cases/decisions/m2690_en.pdf).
(8) Abusleme, J. A.; Gavezotti, P. Suspension (co)polymerization with bis(dichlorofluoroacetyl) peroxide for preparation of hydrogen-containing thermoplastic fluoropolymers. U.S. Patent: 5,569,728, 1995.
(9) Arnold, R. G.; Barney, A. L.; Thompson, D. C. *Rubber Chem. Technol.* **1973**, *46* (3), 619–52.
(10) Jagels, S.,Materials Engineer in Solvay−Solexis; Thorofare, NJ, Personal Communication, 2003.
(11) Stevens, M. P., *Polymer Chemistry: An Introduction*, 3rd ed.; Oxford University Press: New York, 1999.

(12) Humphrey, J. S.; Amin-Sanayei, R. Vinylidene Fluoride Polymers. In *Encyclopedia of Polymer Science and Technology*, 3rd ed.; Mark, H. F., Ed.; Wiley: New York, 2004; Vol. 4, pp 510–533..
(13) Preliminary Risk Assessment: Perfluorooctanic Acid (PFOA) and Fluorinated Telomers; U.S. Environmental Protection Agency: April, 2003.
(14) 2010/15 PFOA Stewardship Program; U.S. Environmental Protection Agency: January, 2006.
(15) Kennedy, K. A.; Roberts, G. W.; DeSimone, J. M. *Adv. Polym. Sci.* **2005**, *175*, 329–346.
(16) Ahmed, T. S.; DeSimone, J. M.; Roberts, G. W. *Macromolecules* **2007**, *40* (26), 9322–9331.
(17) Charpentier, P. A.; DeSimone, J. M.; Roberts, G. W. *Ind. Eng. Chem. Res.* **2000**, *39* (12), 4588–4596.
(18) Charpentier, P. A.; DeSimone, J. M.; Roberts, G. W. *Chem. Eng. Sci.* **2000**, *55* (22), 5341–5349.
(19) Charpentier, P. A.; Kennedy, K. A.; DeSimone, J. M.; Roberts, G. W. *Macromol. Commun.* **1999**, *32* (18), 5973–5975.
(20) Saraf, M. K.; Gerard, S.; Wojcinski, L. M.; Charpentier, P. A.; DeSimone, J. M.; Roberts, G. W. *Macromolecules* **2002**, *35* (21), 7976–7985.
(21) Zhao, C. X.; Zhou, R. M.; Pan, H. Q.; Jin, X. S.; Qu, Y. L.; Wu, C. J.; Jiang, X. K. *J. Org. Chem.* **1982**, *47* (11), 2009–2013.
(22) Liu, T.; Desimone, J. M.; Roberts, G. W. *J. Polym. Sci., Part A: Polym. Chem.* **2005**, *43* (12), 2546–2555.
(23) Liu, T.; DeSimone, J. M.; Roberts, G. W. *Chem. Eng. Sci.* **2006**, *61* (10), 3129–3139.
(24) Liu, T.; Garner, P.; DeSimone, J. M.; Roberts, G. W.; Bothun, G. D. *Macromolecules* **2006**, *39* (19), 6489–6494.
(25) DiNoia, T. P.; McHugh, M. A.; Cocchiaro, J. E.; Morris, J. B. *Waste Management* **1998**, *17* (2–3), 151–158.
(26) Reid, R. C.; Prausnitz, J. M.; Poling, B. E., *The Properties of Gases and Liquids*. 4th ed.; McGraw Hill: New York, 1987.
(27) Thomson, G. H.; Brobst, K. R.; Hankinson, R. W. *AIChE J.* **1982**, *28* (4), 671–676.
(28) Rindfleisch, F.; DiNoia, T. P.; McHugh, M. A. *J. Phys. Chem.* **1996**, *100* (38), 15581–15587.
(29) Isbester, P. K.; Brandt, J. L.; Kestner, T. A.; Munson, E. J. *Macromolecules* **1998**, *31* (23), 8192–8200.
(30) Dohany, J. E., Poly(Vinylidene Fluoride). In *Kirk-Othmer Encyclopedia of Chemical Technology*, *4*th ed.; Kirk-Othmer , Ed. John Wiley and Sons: New York, 1998.
(31) Mueller, P. A.; Storti, G.; Apostolo, M.; Martin, R.; Morbidelli, M. *Macromolecules* **2005**, *38* (16), 7150–7163.
(32) Ahmed, T. S.; DeSimone, J. M.; Roberts, G. W. *Chem. Eng. Sci.* **2004**, *59* (22–23), 5139–5144.
(33) Ahmed, T. S.; DeSimone, J. M.; Roberts, G. W. *Macromolecules* **2006**, *39* (1), 15–18.
(34) Odian, G., *Principles of Polymerization*. 4th ed.; John Wiley and Sons, Inc: New York, 2004.
(35) Matyjaszewski, K.; Davis, T. P. *Handbook of Radical Polymerization*. Wiley-Interscience: New York, 2002.
(36) Ito, K.; O'Driscoll, K. F. *J. Polym. Sci., Polym. Chem. Ed.* **1979**, *17* (12), 3913–3921.
(37) Luft, G.; Ogo, Y., Activation Volumes of Polymerization Reactions. In *Polymer Handbook*, 4th ed.; Brandrup, J., Immergut, E. H., Grulke, E. A., Eds.; John Wiley and Sons: New York, 1999; pp IIII–429.
(38) Gelin, M.-P.; Ameduri, B. *J. Fluorine Chem.* **2005**, *126* (4), 577–585.
(39) Moggi, G.; Bonardelli, P.; Russo, S. *6th Conv. Ital. Sci. Macromol., [Atti]* **1983**, *2*, 405–408.
(40) Logothetis, A. L. *Prog. Polym. Sci.* **1989**, *14* (2), 251–296.
(41) Bonardelli, P.; Moggi, G.; Turturro, A. *Polymer* **1986**, *27* (6), 905–909.
(42) Tai, H.; Wang, W.; Howdle, S. M. *Macromolecules* **2005**, *38* (22), 9135–9142.
(43) Beginn, U.; Najjar, R.; Ellmann, J.; Vinokur, R.; Martin, R.; Moeller, M. *J. Polym. Sci., Part A: Polym. Chem.* **2006**, *44* (3), 1299–1316.
(44) Mayo, F. R.; Lewis, F. M. *J. Am. Chem. Soc.* **1944**, *66* (9), 1594–1601.
(45) Marquardt, D. W. *SIAM J. Appl. Math.* **1963**, *11* (2), 431–441.

MA702526U